Journal of Alloys and Compounds 509 (2011) 5242–5249

Contents lists available at ScienceDirect

Journal of Alloys and Compounds

journal homepage: www.elsevier.com/locate/jallcom

The electronic, mechanical properties and theoretical hardness of chromium carbides by first-principles calculations

Yefei Li[a,*], Yimin Gao[a], Bing Xiao[b], Ting Min[a], Ying Yang[a], Shengqiang Ma[a], Dawei Yi[a]

[a] State Key Laboratory for Mechanical Behavior of Materials, Xi'an Jiaotong University, Xi'an 710049, PR China
[b] Department of Physics and Quantum Theory Group, School of Science and Engineering, Tulane University, New Orleans, LA 70118, USA

ARTICLE INFO

Article history:
Received 14 October 2010
Received in revised form 22 January 2011
Accepted 2 February 2011
Available online 23 February 2011

Keywords:
First-principles calculations
Inorganic compounds
Mechanical properties
Electronic structure
Stability

ABSTRACT

In the present study, the ground state properties of chromium carbides (h-CrC, c-CrC, Cr_3C, Cr_3C_2, Cr_7C_3, and $Cr_{23}C_6$) are calculated by means of the first-principles pseudopotential method using the CASTEP code. The equilibrium crystal structures and thermodynamical stability of the six chromium carbide phases are discussed. Moreover, the chemical bonding in these carbides are interpreted by calculating the density of states, electron density distribution and Mulliken analysis; all the six chromium carbides have a combination of metallic, ionic and covalent bonding characteristic, while Cr_7C_3 exhibits the strongest metallic character. The elastic constants, elastic anisotropies and theoretical hardness of the carbides are also presented, which are important parameters for the structural materials and surface coatings.

1. Introduction

Chromium carbides usually have many applications owing to their properties such as high hardness, high melting point, excellent resistance to chemical corrosion, high moduli and super wear resistance [1,2]. As a result, chromium carbides are often used in surface coatings, which are of great technological importance in the cutting tool industries [3,4]; meanwhile, it is well known that chromium carbides play a significant role in the Fe–Cr–C alloys as the precipitated carbides [5]. Therefore, more and more experimental and theoretical researches have been conducted.

In the Cr–C binary phase diagram there are three solid state phases present: cubic $Cr_{23}C_6$ (space group $Fm\bar{3}m$, melting point 1848 K), orthorhombic Cr_3C_2 (space group *Pnma*, melting point 2083 K) and Cr_7C_3 (space group *Pnma*, melting point 2038 K) [2,6]. Most researches are focused on Cr_3C_2 ceramics [1,7–10]. Loubière et al. [1] prepared Cr_3C_2 powders by the heat-treatment of metastable chromium oxides of controlled morphology in H_2-CH_4 atmosphere; and then, they [7] observed the transformation from Cr_3C_2 to the metastable Cr_3C_{2-x} ($0 \le x \le 0.5$) and also found the high specific surface area ($\geq$210 m^2/g) of the starting oxide is the necessary condition to obtain the metastable Cr_3C_{2-x}. Lately, Ebrahimi-Kahrizsangi et al. [8] synthesized Cr_3C_2, which is the only chromium carbide form, from chromium oxide by reduction with methane. Romero et al. [9] used radio frequency magnetron sputtering method and obtained Cr/CrC multilayers which include quasi-amorphous Cr_3C_2 layers. Recently, Hirota et al. [10] found that Cr_3C_2 ceramics can be synthesized and consolidated simultaneously at 1300 °C for 10 min under 30 MPa from mixtures of Cr and amorphous carbon powders; they exhibit excellent mechanical properties: bending strength σ_b = 690 GPa, Vickers hardness H_V = 18.9 GPa, and fracture toughness K_{IC} = 7.1 MPa $m^{1/2}$. Kleykamp [11] investigated the thermodynamic properties of the three carbides Cr_3C_2, Cr_7C_3 and $Cr_{23}C_6$, and provided that the enthalpies of formation at 298 K which were evaluated to be −72.3 kJ/mol, −144 kJ/mol and −344 kJ/mol for Cr_3C_2, Cr_7C_3 and $Cr_{23}C_6$, respectively.

Although Cr_3C_2, Cr_7C_3, and $Cr_{23}C_6$ are the common phases in most of Cr-based coatings, another two metastable chromium carbides (CrC and Cr_3C) are also obtained in experiments [12–16]. Liu et al. [14] synthesized metastable NaCl-structure CrC by 50 KeV carbon-ion implantation into pure chromium metal films, and proved that the only FCC structure with lattice parameters of 0.403 nm is stable when the temperature is up to 250 °C. Uebing et al. [15] found the surface phases of CrN and CrC that crystallize in the NaCl structure type. In the Cr–C binary system, Cr_3C is a metastable structure; however, the $(Fe, Cr)_3C$ phase is thermodynamically stable in the temperature range of 658–1187 °C, where it has the appearance of a ternary phase in the phase diagram [16].

* Corresponding author at: School of Materials Science and Engineering, Xi'an Jiaotong University, 28 Xianning West Road, Xi'an, Shaanxi Province 710049, PR China. Tel.: +86 29 82665479; fax: +86 29 82665479.
E-mail addresses: yefeili@126.com (Y. Li), ymgao@mail.xjtu.edu.cn (Y. Gao).

0925-8388/$ – see front matter © 2011 Elsevier B.V. All rights reserved.
doi:10.1016/j.jallcom.2011.02.009

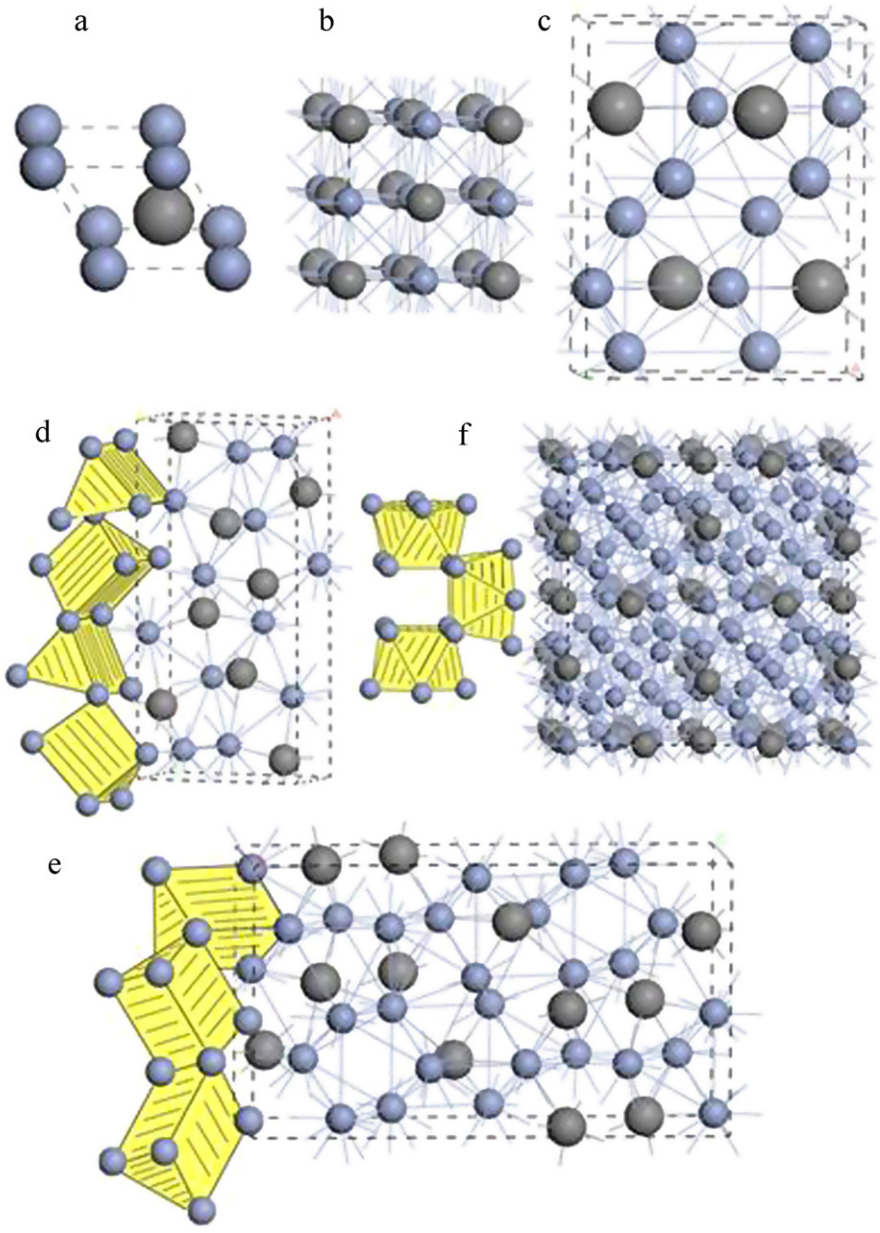

Fig. 1. Crystal structures of the h-CrC (a), c-CrC (b), Cr_3C (c), Cr_3C_2 (d), Cr_7C_3 (e), and $Cr_{23}C_6$ (f) compounds. The large gray balls represent C atoms; the small blue balls refer to Cr atoms. (For interpretation of the references to color in this figure legend, the reader is referred to the web version of the article.)

However, although there are a huge number of experimental studies about the chromium carbides, most of them are about the preparation methods and stabilities of structures. The basic properties such as the thermodynamic and mechanical properties (formation enthalpies, chemical bonding, hardness, elastic anisotropies, etc.), which are of great technological importance, are not very clear. Therefore, theoretical studies on the basic properties of materials have been performed [17–24]. Music et al. [17] have applied the first-principles calculations to study the electronic and mechanical properties of Cr_7C_3 by using an orthorhombic cell; they found covalent-ionic Cr–C–Cr chains in a metallic matrix; the estimated bulk modulus and Young modulus values are 309 and 371 GPa, respectively. Konyaeva et al. [18] investigated the structural, electronic, and magnetic properties of $(Fe, Cr)_7C_3$ within the ab initio calculations. They found that the formation of $(Cr, Fe)_7C_3$ is energetically more favorable than Fe_7C_3, which can explain the $(Cr, Fe)_7C_3 \rightarrow Cr_7C_3$ transformation. Xiao et al. [19] discussed that the chemical stability of $(Fe, Cr)_7C_3$ can be greatly improved by codoping with B, W and Mo impurities. Besides, dos Santos [20] analyzed the electronic structure of $Cr_{23}C_6$ by using LMTO (linear muffin-tin orbital) and LAPW (linear plain and expanded waves) methods; he found that a zero magnetic moment was obtained in LMTO method, while a small magnetic moments in the interstitial region and in the Cr II site were obtained in LAPW method. This may result from the charge transference of Cr II site. Xie et al. [5] investigated the site preference of Fe in $Cr_{23-x}Fe_xC_6$, and they found that Fe atoms preferentially substitute for Cr at 4a sites first and then 8c sites, and the increase in x value is accompanied by the decrease in the thermodynamic stability of $Cr_{23-x}Fe_xC_6$. Zhou et al. [21] calculated the elastic properties and electronic structures of several Cr doped Fe_3C compounds using first-principles method and concluded that Cr_3C is the most stable structure among four $(Fe, Cr)_3C$ structures (Fe_3C, $Fe_{11}Cr_1C_4$, $Fe_{10}Cr_2C_4$ and Cr_3C), but they are less stable than Cr_3C_2, Cr_7C_3 and $Cr_{23}C_6$. Lately, Jiang [22] studied the structural, elastic,

and electronic properties of chromium carbides by first-principles calculations; by providing a set of elastic constants for the first time, he found WC-type CrC is a potential low-compressibility and hard material with the highest bulk and shear moduli and the lowest Poisson's ratio. However, to the best of our knowledge, the theoretical hardness, and elastic anisotropy indexes of chromium carbides have not yet been discussed systematically in literatures. In this paper, all three stable phases in the Cr–C binary phase diagram, two metastable chromium carbides (NaCl type-CrC and Cr_3C with Fe_3C structure) discovered in experiments and WC-type CrC was considered as the potential hard material by Jiang [22] using first-principles calculations; our main purpose is to provide more useful information on the theoretical hardness, elasticity and electronic structures of them.

2. Calculation methods and models

The crystal structures of chromium carbides are shown in Fig. 1. Two different structures of CrC are involved in this article: one is NaCl-structure, which was discovered in experiment [14,15], the other is WC-structure, which was considered as a potential hard material [22]. Cr_3C with Fe_3C-structure is also considered which usually appears in Fe–Cr–C ternary system in the form of cementite. Besides, three kinds of chromium carbides in Cr–C binary system were calculated. They are Cr_3C_2 (*Pnma*), Cr_7C_3 (*Pnma*) and $Cr_{23}C_6$ ($Fm\bar{3}m$): the carbon atoms filled in trigonal Cr_6 prisms are emphasized in Cr_3C_2 and Cr_7C_3 compounds, while they are placed in square antiprisms in $Cr_{23}C_6$ [24]. In Table 1 the cell structures are listed, such as lattice parameters and chromium site. All calculations were carried out by using first-principles method based on density functional theory, as implemented in CASTEP code [25–27]. The ultrasoft pseudo potentials were employed to represent the interactions between ionic core and valence electrons. For Cr and C, the valence electrons considered are $3s^2 3p^6 3d^5 4s^1$, $2s^2 2p^2$, respectively. A special k-point sampling method was used for the integration by setting as $11 \times 11 \times 11$, $11 \times 11 \times 10$, $10 \times 8 \times 10$, $6 \times 10 \times 3$, $6 \times 4 \times 2$, and $5 \times 5 \times 5$ for CrC CrC (WC-structure, simplified as h-CrC), (NaCl-structure, simplified as c-CrC), Cr_3C, Cr_3C_2, Cr_7C_3 and $Cr_{23}C_6$ with Monkhorst–Pack scheme in the first irreducible Brillouin zone [28]. Generalized gradient approximation of PBE approach was used for exchange-correlation energy calculations [29]. A kinetic energy cut-off value of 350 eV was used for plane wave expansions. The total energy changes during the optimization finally converged to less than 1×10^{-6} eV and the forces per atom were reduced to 0.02 eV/Å. The Broyden–Fletcher–Goldfarb–Shannon (BFGS) algorithm was applied to relax the whole structure to reach the ground state where both cell parameters and fractional coordinates of atoms were optimized simultaneously. All calculations were performed with the non-spin polarized density functional theory. The magnetic states of these Cr–C binary compounds were considered to be paramagnetic, and such postulate will only slightly affect the properties discussed in this paper of them.

3. Results and discussion

3.1. Electronic structures

The calculated cell parameters of chromium carbides are given in Table 1. Generally speaking, the calculated lattice parameters of all Cr–C compounds are in good agreement with available experimental results. The average deviation of our results to experimental results for lattice parameters is less than 2%. The values of cohesive energy and formation enthalpy here are calculated within the

Table 1
The calculated cell parameters (a, b, c, in Å; V_{cell} in Å^3), density of states at the Fermi surface (D_f, states/(eV formula)), and metallicity parameter (f_m) of h-CrC, c-CrC, Cr_3C, Cr_3C_2, Cr_7C_3 and $Cr_{23}C_6$.

Species	Space group	Lattice parameters			Chromium site[a]	E_{coh}	$\Delta_f H$	D_f	f_m
		a	b	c					
h-CrC	$P\bar{6}m2$	2.7072.71[a]	–	2.6162.62[a]	1a (0, 0, 0)	−9.75	−0.028	0.373	0.008
c-CrC	$Fm\bar{3}m$	4.0684.03[b]	–	–	4b (0.5, 0.5, 0.5)	−9.56	0.170	1.199	0.026
Cr_3C	*Pnma*	5.1885.12[c]	6.6676.80[c]	4.5214.58[c]	8d (0.1886, 0.0589, 0.3321)	−10.06	−0.088	1.687	0.143
					4c (0.0354, 0.25, 0.8373)				
Cr_3C_2	*Pnma*	5.485 (5.554[d])	2.789 (2.833[d])	11.474 (11.494[d])	4c (0.6312, 0.25, 0.5687)	−9.94	−0.114 (−0.15[e])	1.770	0.150
					4c (0.3186, 0.25, 0.7265)				
					4c (0.9836, 0.25, 0.4018)				
Cr_7C_3	*Pnma*	4.511 (4.526[f], 4.5[a], 4.519[g])	6.903 (7.010[f], 6.93[a], 6.89[g])	12.080 (12.142[f] 12.03[a], 12.102[g])	4c (0.0579, 0.25, 0.6261)	−10.03	−0.112 (−0.149[e])	4.401	0.365
					4c (0.2501, 0.25, 0.2063)				
					4c (0.2619, 0.25, 0.4165)				
					8d (0.0565, 0.0642, 0.8119)				
					8d (0.2509, 0.0657, 0.0218)				
$Cr_{23}C_6$	$Fm\bar{3}m$	10.554 (10.66[b])	–	–	4a (0, 0, 0)	−10.10	−0.087 (−0.123[e])	12.025	0.257
					8c (1/4, 1/4, 1/4)				
					32f (0.3819, 0.3819, 0.3819)				
					48h (0, 0.1699, 0.1699)				

a–g: Refs. [12,14,22,30–34].

[a] The chromium sites used in this paper are according to the Inorganic Crystal Structure Database (ICSD) #57008, #391234, #76799, #62667 for c-CrC, Cr_3C_2, Cr_7C_3 and $Cr_{23}C_6$, respectively. Meanwhile, the chromium sites of h-CrC with WC-structure, and Cr_3C with Fe_3C-structure are considered according to the ICSD #43380, #99027.

following equations:

$$E_{coh}(Cr_xC_y) = E_{tot}(Cr_xC_y) - xE_{iso}(Cr) - yE_{iso}(C) \quad (1)$$

$$\Delta_r H(Cr_xC_y) = E_{coh}(Cr_xC_y) - xE_{coh}(Cr) - yE_{coh}(C) \quad (2)$$

All of the calculated formation enthalpies of these chromium carbides except c-CrC are minus as shown in Table 1, indicating that they are thermodynamically stable. By observing the values of formation enthalpy, one could conclude that the stability sequence is $Cr_3C_2 > Cr_7C_3 > Cr_3C \approx Cr_{23}C_6 >$ h-CrC > c-CrC. The positive formation enthalpy of NaCl-structure CrC may be the reason why CrC with NaCl-structure has been observed in the non-equilibrium condition and is only stabilized up to about 250 °C [14].

Three parameters are used to indicate the electronic structures and chemical bonding characteristics of all Cr–C phases, which are the partial density of states (PDOS), electron density distribution map and Mulliken population analysis.

Although the electronic structures of chromium carbides have been analyzed via first-principles calculations (see Ref. [17,22,30]), we present here a brief review and summation of these properties, then give further discussions about the electronic structures of the six chromium carbides by means of partial density of states, electron density distribution maps, metallicity and Milliken population analysis, etc. Generally, the bonding in chromium carbides can be classified as a combination of metallic, ionic, and covalent characters. The metallic aspect can be attributed to the partially filled Cr 3d bands, as illustrated in the PDOS (Fig. 2). Further evidence of metallic bonding is presented in total electron density distribution map (Fig. 3), where the electron density values are greatly larger than zero even in the interstitial regions. Besides, the metallicity of the compounds can be estimated by:

$$f_m = \frac{n_m}{n_e} = \frac{k_B T D_f}{n_e} = \frac{0.026 D_f}{n_e} \quad (3)$$

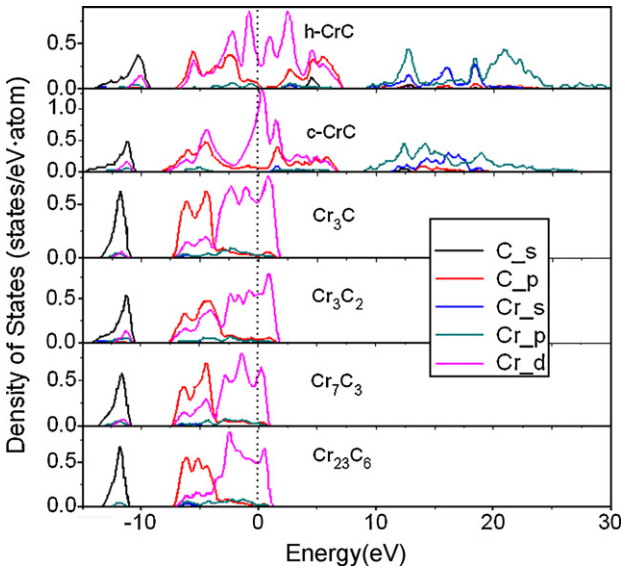

Fig. 2. Partial density of states of chromium carbides. The dot lines represent the position of the Fermi surface.

where D_f is the DOS value at the Fermi level in unit states/eV cell, and T is the temperature; n_m and n_e are the thermal excited electrons and valence electron density of the cell, respectively; k_B is the Boltzmann constant. n_e is calculated by $n_e = N/V_{cell}$, N is the total number of valence electrons and V_{cell} is the cell volume. The related parameters and calculation results are shown in Table 1, from which we can observe that f_m decreases in the following sequence: $Cr_7C_3 > Cr_{23}C_6 > Cr_3C_2 > Cr_3C >$ c-CrC > h-CrC. Thus, the maximal "metallicity" corresponds to Cr_7C_3 and the minimal one is h-CrC. In Fig. 2, the p bands of C atoms are overlapped with the

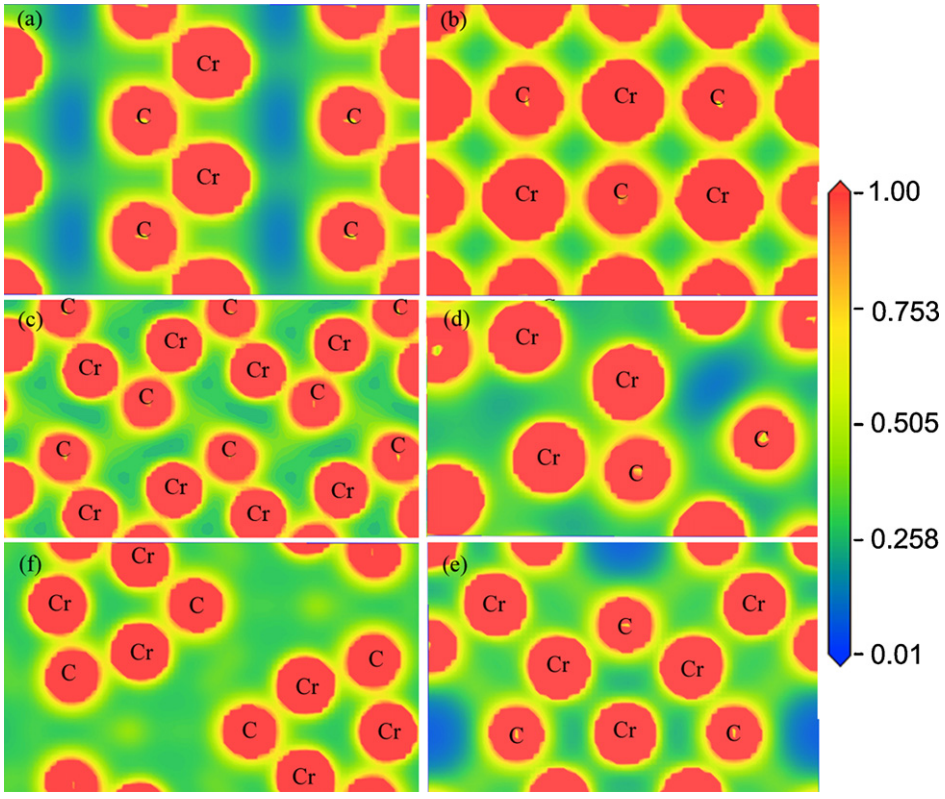

Fig. 3. Total electron density distribution through (1 1 0), (0 1 0), (0 1 0), (0 1 0), (1 0 0) and (0 1 0) slice intersecting both Cr and C atoms for h-CrC (a), c-CrC (b), Cr_3C (c), Cr_3C_2 (d), Cr_7C_3 (e) and $Cr_{23}C_6$ (f), respectively. The electron density contours were plotted from 0.01 to 1.0 e/Å^3.

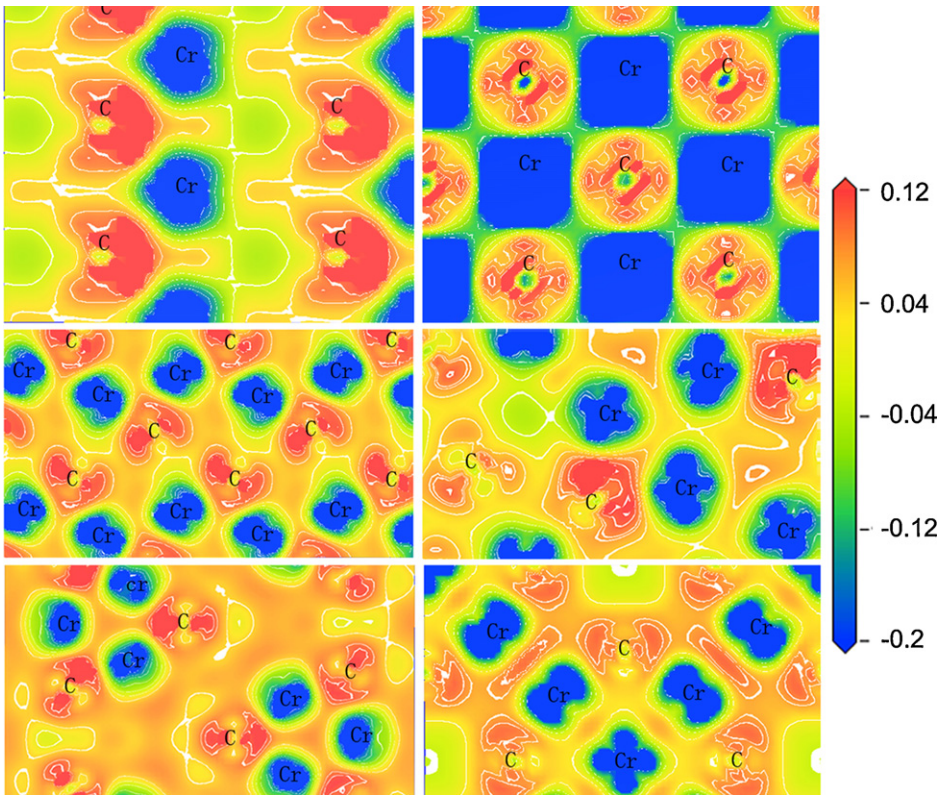

Fig. 4. Electron density difference distribution (relative to the isolated atoms) through (1 1 0), (0 1 0), (0 1 0), (0 1 0), (1 0 0) and (0 1 0) slice for h-CrC (a), c-CrC (b), Cr_3C (c), Cr_3C_2 (d), Cr_7C_3 (e) and $Cr_{23}C_6$ (f) plotted from −0.2 to 0.12 e/Å^3, respectively.

d bands of Cr atoms, which illustrate p–d hybridization between C and Cr atoms forming covalent bonding. However, the centre of gravity of C-p bonds does not completely coincide with the Cr-d bands, which, to some extent, indicates the ionic bonding in these carbides. The electron density difference maps, which are defined as the electron density difference between the isolated atoms and their bonding states, reflect directly their ionic nature (Fig. 4). Another powerful evidence for covalent bond is the higher densities along the C–Cr bonds in Fig. 3 and the distorted contours in Fig. 4. Therefore, the Cr–C–Cr covalent chains discovered in Cr_7C_3 by Music [17] also appear in other chromium carbides.

The stability of the two polymorphs of CrC can be explained both by energies and electronic structures. As shown in Table 1, the calculated cohesive energy and formation enthalpy of h-CrC are smaller than c-CrC; in addition, the partial density of states of them clearly indicate that the Fermi surface is dominated by d bands of Cr atoms in the two crystal structures, and the splitting of d bands is actually determined by the configurations of Cr sublattice. In h-CrC, we can observe a small pseudo-gap close to the Fermi level. The previous calculations on TiC and WC cubic and hexagonal polymorphs revealed that in hexagonal phase this pseudo-gap is caused by the d–d interactions between metal atoms. Below the first sharp peak near the top of valence band, we can see another gap which is attributed to the covalent bonding between Cr and C atoms. On the other hand, for cubic-phase, a large pseudo-gap can be clearly seen in Fig. 2. In contrary to hexagonal phase, this large splitting of d bands is directly related to the covalent interactions of Cr–C bonds. The hexagonal phase is stabilized in WC, but in the case of TiC, the ground state is cubic phase. These results can be easily explained by the rigid band theory if it is applicable for these polymorphs. Since the number of d electrons in W, Cr and Ti is different, there are less electrons in 3d orbital of Ti, then TiC favors NaCl-type structure in energy; for WC, adopting NaCl structure will increase the DOS value at the Fermi level greatly, thus destabilizing the crystal structure, and in hexagonal phase, the large peak at the Fermi level in cubic phase now is split because of strong d–d metallic bonds. Therefore, WC has a hexagonal cell as the ground state. Similarly, CrC also adopts hexagonal cell which is lower in energy than cubic phase; otherwise there are more electrons in 3d orbital of Cr than that of TiC, the extra electrons will shift the Fermi level upward and above the large pseudo-gap in cubic phase, and as can be seen from Fig. 2, the DOS value at the Fermi level for cubic CrC is close to 0.7 electrons/eV, and which is obviously larger than hexagonal phase. In summary, the stability of CrC polymorphs is mainly determined by the electronic interactions of Cr sublattice. The covalent Cr–C bonds in the two phases are not significantly affected by the structural changes.

Population analysis results can provide more insightful information on chemical bonding, which are listed in Table 2. Mulliken method is applied for the overlap population and the charge calculations. Eqs. (4) and (5) are used to calculate the average bond length and the average overlap population:

$$\overline{L}(\mathrm{AB}) = \frac{\sum L_i N_i}{\sum N_i} \tag{4}$$

$$\overline{n}(\mathrm{AB}) = \frac{\sum n_i N_i}{\sum N_i} \tag{5}$$

Here $\overline{L}$(AB) and $\overline{n}$(AB) represent the average bond length and the mean bond population, respectively; N_i is the total number of i bond in the cell and L_i is the bond length of i type.

First of all, we want to list the electronegativity values of Cr and C atoms in Pauling scale: 2.55 (C), 1.66 (Cr). As shown in Table 2, the largest positive charges are carried by Cr atoms of CrC in NaCl-structure, indicating the stronger ionicity in this compound; C atoms carry the negative charges for all chromium carbides; and the value varies from −0.40 (h-CrC) to −0.59 ($Cr_{23}C_6$). One can assume three possible electron transfer paths intra or inter the C

Table 2
Mulliken population analysis results of all Cr–C compounds: $\bar{n}$ is average population, $\bar{L}$ is average bonding length. Note that total charges of s and p orbitals of C are calculated as 3s + 4s and 3p + 4p, respectively.

Carbides	Species (ion)	s	p	d	Total electrons	Charges (e)
h-CrC	C	1.40	3.00		4.40	−0.40
	Cr	2.20[a]	6.44[b]	4.96	13.60	0.40
c-CrC	C	1.43	3.06		4.48	−0.48
	Cr	2.09[a]	6.47[b]	4.96	13.52	0.48
Cr_3C	C	1.38	3.18		4.56	−0.56
	Cr	2.10[a]	6.72[b]	4.99	13.81	0.19
Cr_3C_2	C	1.40	3.10		4.50	−0.50
	Cr	2.14[a]	6.55[b]	4.98	13.67	0.33
Cr_7C_3	C	1.38	3.15		4.53	−0.53
	Cr	2.10[a]	6.69[b]	4.99	13.77	0.23
$Cr_{23}C_6$	C	1.38	3.20		4.59	−0.59
	Cr	2.12[a]	6.74[b]	4.99	13.85	0.15

Carbides	Bond	$\bar{n}$ (Electrons)	$\bar{L}$ (Å)
CrC (WC)	C–Cr	0.31	2.04
CrC (NaCl)	C–Cr	0.32	2.03
Cr_3C	C–Cr	0.26	2.12
	Cr–Cr	0.10	2.58
Cr_3C_2	C–Cr	0.34	2.11
	Cr–Cr	0.04	2.63
Cr_7C_3	C–Cr	0.28	2.14
	Cr–Cr	0.07	2.58
$Cr_{23}C_6$	C–Cr	0.29	2.10
	Cr–Cr	0.15	2.56

[a] 3s + 4s.
[b] 3p + 4p.

and Cr atoms. The first one refers to p-d hybridized covalent bonding between C and Cr, which can be designated as 3d + 4s (Cr) to 2p (C) for all Cr–C compounds; the second one is induced by the metallic bonding among Cr atoms through d–d or s–d interactions; the third one is the electron transfer from 4s bonds of Cr atoms to 2p bonds of C atoms because of the different electronegativity values of C and Cr atoms. Besides, according to Hund's rule, the half-occupied d-orbitals are inert; therefore, all of the d-bonds of Cr almost have 5 electrons. In c-CrC, the Cr atoms carrying the largest positive charges and the shortest length of Cr–C bonds, this will deduce that c-CrC could be expected to have more ionic character than others.

3.2. Mechanical properties

The mechanical properties of the studied Cr–C binary compounds, such as elastic moduli, elastic anisotropy and theoretical hardness, play an important role in the wear resistance of surface coating materials. Many elastic properties of material are directly correlated to the full set elastic constants. Therefore, we calculated the elastic constants of Cr–C binary compounds first. In CASTEP code, the elastic constants were obtained by fitting the Hooker's law to the deformed crystal structures; thus, a stress–strain approach was employed to calculate elastic constants. The main advantage of this method is that the required strain patterns can be greatly reduced for the low symmetry crystal structures which usually have large number independent elastic constants. The bulk modulus (B_{VRH}), shear modulus (G_{VRH}) for polycrystalline crystal can be estimated within Voigt-Reuss-Hill methods [35] after evaluating the elastic constants; then the Young's modulus and Poisson's ratio can be calculated as follows [36]:

$$E = \frac{9B_{VRH}G_{VRH}}{3B_{VRH} + G_{VRH}} \quad (6)$$

$$\upsilon = \frac{3B_{VRH} - 2G_{VRH}}{2(3B_{VRH} + G_{VRH})} \quad (7)$$

The calculated elastic constants of these Cr–C binary compounds are shown in Table 3. For two CrC polymorphs, most

Table 3
Calculated values for elastic constants (C_{ij}), bulk modulus (B, in GPa), shear modulus (G, in GPa), Young's modulus (E, in GPa), Poisson's ratio (υ) and universal elastic anisotropy index of h-CrC, c-CrC, Cr_3C, Cr_3C_2, Cr_7C_3 and $Cr_{23}C_6$.

Species	C_{11}	C_{12}	C_{13}	C_{22}	C_{23}	C_{33}	C_{44}	C_{55}	C_{66}
h-CrC	572.4	164.0	196.7	572.4	196.7	771.8	279.3	279.3	204.2
c-NaCl	585.9	183.6					131.9		
Cr_3C	518.7	195.3	208.4	445.6	212.2	401.6	114.8	193.9	202.3
Cr_3C_2	447.1 (484[a])	217.5 (229[a])	243.3 (243[a])	545.3 (554[a])	217.9 (244[a])	471.2 (491[a])	237.7 (230[a])	116.6 (111[a])	241.3 (235[a])
Cr_7C_3	410.1 (409[a])	241.1 (252[a])	203.7 (227[a])	441.1 (376[a])	257.3 (333[a])	459.5 (409[a])	168.5 (145[a])	124.3 (123[a])	108.3 (82[a])
$Cr_{23}C_6$	473.8 (481[a], 487[b])	186.6 (209[a], 200[b])					146.7 (138[a], 149[b])		

Species	B	G	B/G	E	ν	G^V/G^R	B^V/B^R	A^U
h-CrC	332.8	240.2	1.39	580.9	0.21	1.02	1.02	0.15
c-CrC	317.7 (327[c])	156.3	2.03	402.8	0.29	1.04	1.00	0.22
Cr_3C	287.5(293[a], 298.2[d])	146.8	1.96	376.3 (358.0[d])	0.28	1.08	1.01	0.39
Cr_3C_2	312.9 (329[a], 333[c])	162.1 (162[a])	1.93	414.7 (416[a], 373.1[b])	0.28 (0.29[a])	1.12	1.00	0.62
Cr_7C_3	300.6 (312[a], 311.7[e], 309[f], 315[c])	118.0 (82[a], 143.9[f])	2.55	313.0 (226[a], 374[e], 371[f])	0.33 (0.38[a])	1.05	1.01	0.25
$Cr_{23}C_6$	282.3 (300[a], 294[c])	145.4 (137[a])	1.94	372.3 (357[a])	0.28 (0.30[a])	1.0001	1.00	0.00053

a–f: Refs. [22,17,23,21,45].

Table 4
Calculated hardness (H_V, GPa) and related parameters of Cr–C compounds: bond density (b_{Cr-C}/Ω), bond strength (S_{Cr-C}), the correction coefficient (f_e).

Phases	b_{Cr-C}/Ω	S_{Cr-C}			f_e	H_V (GPa)	H_v^{Exp} (GPa)
		Max	Min	Aver			
h-CrC	0.361	0.062	0.062	0.062	0.001	32.1	
c-CrC	0.356	0.062	0.062	0.062	0.001	31.7	
Cr3C	0.145	0.128	0.125	0.126	0.107	19.6	
Cr3C2	0.262	0.128	0.0713	0.079	0.270	20.9	10.2–18.3[a], 18.9[b], 18–25[c]
Cr7C3	0.185	0.129	0.083	0.092	0.107	18.3	16.9[d], 17[b], 16[e]
Cr23C6	0.163	0.091	0.062	0.075	0.107	13.2	15[b]

a–e: Experimental data from Refs. [19,10,50,51,52].

elastic constants of c-CrC are larger than h-CrC, the only exception is the C_{44} which represents the shear modulus on (0 0 1) crystal plane, the value of C_{44} for c-CrC is only one half of hexagonal phase, for example the values are 279.3 GPa and 131.9 GPa for h- and c-CrC, respectively. As a result, the calculated average elastic properties of c-CrC are less remarkable than h-CrC. The same reason can be used to explain the results of other chromium carbides; the average moduli are sensitive to the shearing elastic constants; for example, Cr_3C has the largest C_{11} (518.7 GPa) and smallest C_{44} (114.8 GPa), the bulk modulus (287.5 GPa) is only comparable to $Cr_{23}C_6$ (282.3 GPa) which also has a rather small C_{44} (146.7 GPa). We also compared our results with other theoretical calculations, they are generally in agreement with each other, and however, for Cr_7C_3 the deviations for some elastic constants (C_{22}, C_{23} and C_{33}) are significant. One possible explanation is the optimized crystal structure of Cr_7C_3 in this work is different to Ref. [22]; as shown in Table 1, the calculated lattice parameters of Cr_7C_3 for b and c are slightly smaller than in the Ref. [22]; thus, most elastic constants are larger than the results in the reference.

Bulk modulus reflects the compressibility of the solid under hydrostatic pressure. The bulk modulus are 332.8, 317.7, 287.5, 312.9, 300.6 and 282.3 GPa for h-CrC, c-CrC, Cr_3C, Cr_3C_2, Cr_7C_3 and $Cr_{23}C_6$, respectively. All of them exhibit larger values than many other common carbides such as Fe_3C (276 [37], 226.8 [38]), TiC (249 [39], 242 [40]), and TiB_2 (213 [41]), but smaller than diamond (436.8 [42]) and WC (400.9 [43]). The h-CrC shows the largest value in these six carbides due to its strong Cr–C, and c-CrC has the second largest bulk modulus. The Poisson's ratios (υ) of the compounds except h-CrC (0.21) range from 0.28 to 0.33, which are near 0.3 and clearly illustrate the strong metallic character of them; and this is consistent with the previous discussions in this paper. The shear modulus (G) is calculated and the values are 240.2, 156.3, 146.8, 162.1, 118.0 and 145.4 GPa for h-CrC, c-CrC, Cr_3C, Cr_3C_2, Cr_7C_3 and $Cr_{23}C_6$, respectively, and Cr_3C_2 has the largest value. In addition, the ratio of B/G is frequently used to indicate the ductility of the compound. It is supposed that for the brittle compound, B/G is smaller than 1.75 (for diamond $B/G = 0.8$) and for metallic compound B/G is greater than 1.75 (for Al $B/G = 2.74$). In our case, the calculated results clearly imply that Cr_7C_3 is more ductile than other chromium carbides, while the value of h-CrC is smallest (1.39), indicating its brittle nature. This is a good illustration of the more remarkable metallicity in Cr_7C_3 and the relatively strong covalence in h-CrC. Besides, h-CrC is considered as a potential hard material [22], but its obvious brittle nature could deteriorate the average mechanical properties at the same time.

All single crystals in practice are anisotropic, so an appropriate parameter to characterize the extent of anisotropy is needed. Recently, Ranganathan and Ostoja-Starzewski [44] summarized the existing anisotropy theories, and concluded that most of them lack universality because of their non-uniqueness and ignoring a large part of the elastic stiffness tensor. Then they developed a new universal anisotropy index, A^U, which can be calculated by the equation below:

$$A^U = 5\frac{G^V}{G^R} + \frac{B^V}{B^R} - 6 \tag{8}$$

where G^V, B^V, G^R and B^R are the shear modulus and bulk modulus estimated within Vogit and Reuss methods, respectively. The anisotropy index of the chromium carbides are listed in Table 3. From this table, we can conclude that: first of all, the values of G^V/G^R and B^V/B^R for all Cr–C carbides are distributed around one ($G^V/G^R \approx 1, B^V/B^R \approx 1$), which means they may be locally isotropic crystals not matter with their crystal class. Secondly, Voigt and Reuss methods give the more close values for bulk modulus than for shear modulus, the difference between Voigt and Reuss methods for shear modulus affects the A^U significantly; finally, the elastic anisotropy decreases in the following sequence: $Cr_3C_2 > Cr_3C > Cr_7C_3 >$ c-CrC > h-CrC > $Cr_{23}C_6$. That is to say, Cr_3C_2 behaves more anisotropy than others; and c-CrC has a larger A^U value than the h-CrC indicating its significant anisotropic property.

The hardness of material plays an important role in its applications, especially used as an abrasive resistant phase [46]. Thus, it is necessary to investigate the hardness of chromium carbides due to its foundation status in the wear resistance materials. According to Šimůnek's theory [47], the theoretical hardness of single crystal can be calculated by a semiempirical approach within the following forms:

$$H = \frac{C}{\Omega} n \left[\prod_{i,j=1}^{n} b_{ij} s_{ij}\right]^{1/n} e^{-\sigma f_e} \tag{9}$$

$$f_e = 1 - \left[\frac{k(\prod_{i=1}^{k} e_i)^{1/k}}{\sum_{i=1}^{k} e_i}\right]^2 \tag{10}$$

$$s_{ij} = \frac{\sqrt{e_i e_j}}{n_i n_j d_{ij}} \tag{11}$$

where n_i and n_j are coordination numbers of atoms i and j, respectively; d_{ij} is the interatomic distance of atoms i and j; the reference energy $e_i = Z_i/R_i$, which represents the potential of the individual atom i to attract crystal valence charge; Z_i is the valence electron number of the atom i, and R_i is the ionic radius of the atom published in Pearson's tables [48]; k corresponds to the number of different atoms in the system; s_{ij} is the strength of the individual bond between atoms i and j; b_{ij} is the number of interatomic bonds between atoms i and j in the unit cell; Ω is the volume of the cell; The semiempirical constant C equals to 1450 coupling the calculated and experimental values; $e^{-\sigma f_e}$ (varies from 0 to 1) modifies the effect of the difference between reference energies (e_i, e_j), and σ equals to 2.8. By using Eqs. (9)–(11) we have calculated the hardness of chromium carbides as shown in Table 4. The values of hardness are 32.1, 31.7, 19.6, 20.8, 18.2 and 13.2 GPa for h-CrC, c-CrC, Cr_3C, Cr_3C_2, Cr_7C_3 and $Cr_{23}C_6$, respectively; the calculated results of the last three carbides satisfactorily agree with the previous literature

conducted by Hirota [10]. To the best of our knowledge, the hardness of h-CrC, c-CrC and Cr_3C is still not very clear, so we may provide some useful information on it. Just as Eqs. (9)–(11), the values of calculated hardness are determined by bond density, bond strength, and the correction coefficient ($e^{-\sigma f_e}$); therefore, we want to illuminate the difference mainly by these three parameters here. In all of the six chromium carbides, there are two kinds of bonds, namely Cr–C and Cr–Cr bonds. Compared with Cr–C bonds, Cr–Cr bonds can be negligible because of the long bond length and weak bond strength (shown in Table 2), therefore, only Cr–C bonds are considered for hardness calculations. Meanwhile, different structures have different numbers and types of Cr–C bonds per Cr atom. For example, there are only two kinds of Cr–C bonds in Cr_3C structure, while $Cr_{23}C_6$ has three kinds of Cr–C bonds. Generally, the compound with high bond density and large bond strength will have high hardness.

The values of hardness of all calculated chromium carbides form the following sequence: $Cr_{23}C_6 < Cr_3C < Cr_7C_3 < Cr_3C_2 <$ c-CrC < h-CrC. It can be seen that to some extent, the hardness of the Cr–C system compounds will be enhanced as increasing the C atoms. The different hardness values between two CrC structures are mainly due to the different bond densities. Hexagonal CrC has a larger bond density than cubic phase, and they have the similar bond strength; thus, the hardness of h-CrC is slightly bigger than c-CrC. Besides, the two CrC polymorphs have larger bond densities and smaller ionic correction coefficient than other Cr–C binary compounds; although Cr–C bonds of them are relatively small, the calculated values of hardness are significantly higher than other phases. $Cr_{23}C_6$ has the lowest hardness (H_V = 13.2 GPa) because of its small bond density and bond strength. This value is just slightly higher than the hardness of pure chromium (H_V = 10.6 GPa [49]). In addition, we have calculated the hardness of h-WC (H_V = 22 GPa [43]) which has the similar structure as h-CrC; the difference of hardness between them clearly indicates that the hardness is greatly affected by the atomic radius (both of Cr and W atoms belong to VIB); the smaller radius gives higher hardness of h-CrC. For Cr_3C_2, Cr_7C_3 and $Cr_{23}C_6$, the calculated hardness values are in good agreement with the experimental results.

4. Conclusions

In the present work, we investigated the properties of the six chromium carbides by using the first-principles calculations method implemented in CASTEP code. The calculated lattice parameters are in good agreement with the experimental results; the thermodynamic stability decreases in the sequence of $Cr_3C_2 > Cr_7C_3 > Cr_3C \approx Cr_{23}C_6 >$ h-CrC > c-CrC, and the positive value of formation enthalpy for c-CrC can explain its metastable nature. All of the carbides show a mixed character of metallic, covalent and ionic bonds. The stability of h-CrC can be explained based on the electronic structures of Cr sub-lattices in cubic and hexagonal phases. The calculated elastic constants indicate that h-CrC has higher elastic moduli; but this phase is more brittle than other carbides because of smallest B/G ratio. The values of G^V/G^R and B^V/B^R for all these Cr–C carbides are distributed around one ($G^V/G^R \approx 1$, $B^V/B^R \approx 1$), indicating that they are locally isotropic crystals not matter with their crystal class. By using Šimůnek's theory, the calculated theoretical values of hardness are consistent with the current experimental results for Cr_3C_2, Cr_7C_3 and $Cr_{23}C_6$. The hardness of the two CrC phases is notably higher than other phases; they could be used as the wear resistance coatings.

Acknowledgments

The authors thank Prof. Y.H. Chen for providing a SGI working station and the CASTEP code. This research is supported by the Natural Science Foundation of China (No. 50872109), the 863 project in China (No. 2009AA03Z524), the Cooperation Foundation for Industry, University and Research Institute, Guangdong Province and Ministry of Education of China (No. 2008B090500242), and the Economic and Trade Commission Creative Technology Program, Guangdong Province of China (No. 200872215).

References

[1] S. Loubière, C. Laurent, J.P. Bonino, A. Rousset, Mater. Res. Bull. 30 (1995) 1535–1546.
[2] M. Cekada, P. Panjan, M. Macek, P. Smid, Surf. Coat. Technol. 151–152 (2002) 31–35.
[3] Y.N. Kok, P.E. Hovsepian, Surf. Coat. Technol. 201 (2006) 3596–3605.
[4] F.J. Cheng, Y.S. Wang, T.G. Yang, Mater. Charact. 59 (2008) 488–492.
[5] J.Y. Xie, N.X. Chen, L.D. Teng, S. Seetharaman, Acta Mater. 53 (2005) 5305–5312.
[6] R.G. Coltters, G.R. Belton, Metall. Mater. Trans. B 15 (1984) 517–521.
[7] S. Loubière, Ch. Laurent, J.P. Bonino, A. Rousset, J. Alloys Compd. 243 (1996) 59–66.
[8] R. Ebrahimi-Kahrizsangi, H.M. Zadeh, V. Nemati, Int. J. Refract. Met. Hard Mater. 28 (2010) 412–415.
[9] J. Romero, A. Lousa, E. Martínez, J. Esteve, Surf. Coat. Technol. 163–164 (2003) 392–397.
[10] K. Hirota, K. Mitani, M. Yoshinaka, O. Yamaguchi, Mater. Sci. Eng. A 399 (2005) 154–160.
[11] H. Kleykamp, J. Alloys Compd. 321 (2001) 138–145.
[12] A. Inoue, T. Masumoto, Scripta Mater. 13 (1979) 711–715.
[13] E. Bouzy, E. Buer-Grosse, G.L. Caër, Philos. Mag. B 68 (1993) 619–638.
[14] B.X. Liu, X.Y. Cheng, J. Phys.: Condens. Matter 4 (1992) L265–L268.
[15] C. Uebing, V. Scheuch, M. Kiskinova, H.P. Bonzel, Surf. Sci. 321 (1994) 89–99.
[16] J.O. Andersson, Metall. Mater. Trans. A 19 (1988) 627–636.
[17] D. Music, U. Kreissig, R. Mertens, J.M. Schneider, Phys. Lett. A 326 (2004) 473–476.
[18] M.A. Konyaeva, N.I. Medvedeva, Phys. Solid State 51 (2009) 2084–2089.
[19] B. Xiao, J. Feng, C.T. Zhou, J.D. Xing, X.J. Xie, Y.H. Chen, Chem. Phys. Lett. 459 (2008) 129–132.
[20] A.V. dos Santos, Physica B 387 (2007) 136–142.
[21] C.T. Zhou, B. Xiao, J. Feng, J.D. Xing, X.J. Xie, Y.H. Chen, R. Zhou, Comput. Mater. Sci. 45 (2009) 986–992.
[22] C. Jiang, Appl. Phys. Lett. 92 (2008) 041909.
[23] K.O.E. Henriksson, N. Sandberg, J. Wallenius, Appl. Phys. Lett. 93 (2008) 191912.
[24] R. Berkane, J.C. Gachon, J. Charles, J. Hertz, Calphad 11 (1987) 375–382.
[25] M.D. Segall, J.D. Philip, M.J. Lindan, C.J. Probert, P.J. Pickard, S.J. Hasnip, M.C. Clark, Payne, J. Phys.: Condens. Matter 14 (2002) 2717–2744.
[26] A.E. Mattsson, P.A. Schultz, M.P. Desjarlais, T.R. Mattsson, K. Leung, Modell. Simul. Mater. Sci. Eng. 13 (2005) R1–R13.
[27] L.Z. Cao, J. Shen, N.X. Chen, J. Alloys Compd. 336 (2002) 18–28.
[28] H.J. Monkhorst, J.D. Pack, Phys. Rev. B 13 (1976) 5188–5192.
[29] J.P. Perdew, K. Burke, Y. Wang, Phys. Rev. B 54 (1996) 16533–16539.
[30] B. Xiao, J.D. Xing, J. Feng, Y.F. Li, C.T. Zhou, W. Su, X.J. Xie, Y.H. Cheng, Physica B 403 (2008) 2273–2281.
[31] J. Glaser, R. Schmitt, H.-J. Meyer, Z. Naturforsch. B: Chem. Sci. 58 (2003) 929–933.
[32] L.D. Teng, K.G. Lu, R.E. Aune, S. Seetharaman, Metall. Mater. Trans. A 35 (2004) 3673–3680.
[33] M.A. Rouault, P. Herpin, M.R. Fruchart, Ann. Chim. 5 (1970) 461–470.
[34] H.L. Yakel, Acta Crystallogr. B: Struct. Sci. 43 (1987) 230–238.
[35] W. Zhou, L.J. Liu, B.L. Li, P. Wu, Q.G. Song, Comput. Mater. Sci. 46 (2009) 921–931.
[36] Z.J. Wu, E.J. Zhao, H.P. Xiang, X.F. Hao, X.J. Liu, J. Meng, Phys. Rev. B 76 (2007) 054115.
[37] M. Nikolussi, S.L. Shang, T. Gressmann, A. Leineweber, E.J. Mittemeijer, Y. Wang, Z.K. Liu, Scripta Mater. 59 (2008) 814–817.
[38] J.H. Jang, I.G. Kim, H.K.D.H. Bhadeshia, Comput. Mater. Sci. 44 (2009) 1319–1326.
[39] Y. Yang, H. Lu, C. Yu, J.M. Chen, J. Alloys Compd. 485 (2009) 542–547.
[40] J.J. Gilman, B.W. Roberts, J. Appl. Phys. 32 (1961) 1405.
[41] Z.L. Liu, X.R. Chen, Y.L. Wang, Physica B 381 (2006) 139–143.
[42] Y.C. Liang, W.L. Guo, Z. Fang, Acta Phys. Sin. 56 (2007) 4847–4855.
[43] Y.F. Li, Y.M. Gao, B. Xiao, T. Min, Z.J. Fan, S.Q. Ma, L.L. Xu, J. Alloys Compd. 502 (2010) 28–37.
[44] S.I. Ranganathan, M. Ostoja-Starzewski, Phys. Rev. Lett. 101 (2008) 055504.
[45] https://www.memsnet.org/material/chromiumcarbidecr3c2bulk/.
[46] R.C.D. Richardson, Wear 10 (1967) 291–309.
[47] A. Šimůnek, Phys. Rev. B 75 (2007) 172108.
[48] W.B. Pearson, The Crystal Chemistry and Physics of Metals and Alloys, Wiley, New York, 1972, pp.151.
[49] http://en.wikipedia.org/wiki/Chromium.
[50] A. Jellad, S. Labdi, T. Benameur, J. Alloys Compd. 483 (2009) 464–467.
[51] H. Motono, M. Yoshinaka, K. Hirota, O. Yamaguchi, J. Jpn. Soc., Powder Powder Metall. 50 (2003) 372–376.
[52] J. Esteve, J. Romero, M. Gómez, A. Lousa, Surf. Coat. Technol. 188–189 (2004) 506–510.